Supporting Information

Materials and Methods

Plant Materials and Growth Conditions

The wild-type *Arabidopsis thaliana* used in this study is of the Landsberg *erecta* (L*er*) ecotype, unless otherwise indicated. The *phyA-1* (1) is in the L*er* ecotype, *phyA-300D* (2), *fhy1-3 fhl-1* (3), *hy5-215* (4), phyA-NLS-GFP *phyA-211* (5) and phyA(Y242H)-NLS-YFP *phyA-211* (6) are in the Col ecotype, *phyA-105* (7) is in the RLD ecotype, *fhy3-4 far1-2* (8) is in the No-0 ecotype. All of these mutants have been described previously. The growth conditions and light sources were as described previously (9). The fluence rates of the light growth chambers (Percival Scientific) were 50 μmol m^{-2} s^{-1} for white light, 24 μmol m^{-2} s^{-1} for far-red light and 12 μmol m^{-2} s^{-1} for red light.

Plasmid Construction

The pCF225 vector (*PHYAp:PHYA-ST2*) was described previously (10). To generate the constructs expressing various mutant forms of phyA, the QuikChange site-directed mutagenesis kit (Stratagene) was employed using pCF225 as template to produce the constructs expressing S590A, T593A, S602A, S590A S602A, S590A T593A S602A (referred to as $phyA^{AAA}$), S590D, T593D, S602D, and S590D T593D S602D (referred to as $phyA^{DDD}$) mutant phyA proteins, respectively. The wild-type phyA protein expressed by the pCF225 vector is referred to as $phyA^{WT}$ in this study.

To generate the constructs expressing $phyA^{WT}$-GFP, $phyA^{AAA}$-GFP and $phyA^{DDD}$-GFP, the pCF225 vector was first cut with *Xba*I and *Bam*HI to release the *PHYA-ST2* coding sequence. Then, the coding sequences of $PHYA^{WT}$, $PHYA^{AAA}$ and $PHYA^{DDD}$ were amplified by PCR using the respective mutant constructs listed above as templates and the primer pairs listed in Table S2. The amplicons were digested with *Spe*I and *Bam*HI and ligated into the pCF225 vector digested with *Xba*I and *Bam*HI, producing *PHYAp:PHYA*^{WT}, *PHYAp:PHYA*^{AAA}, and *PHYAp:PHYA*^{DDD}, respectively. The reverse primer used to amplify the coding sequences of $PHYA^{WT}$, $PHYA^{AAA}$ and $PHYA^{DDD}$ contains a *Not*I site upstream of the *Bam*HI site, therefore the *Not*I site was introduced

into the respective constructs. Finally, the *GFP* coding sequence was amplified by PCR using *35S:GFP-FHY1* (11) as template and the primer pairs listed in Table S2, and then cloned into the *Not*I-*Bam*HI sites of *PHYAp:PHYA*^{WT}, *PHYAp:PHYA*^{AAA} and *PHYAp:PHYA*^{DDD}, producing *PHYAp:PHYA*^{WT}*-GFP*, *PHYAp:PHYA*^{AAA}*-GFP* and *PHYAp:PHYA*^{DDD}*-GFP*, respectively.

To generate the constructs expressing phyA^{WT}-NLS-GFP, phyA^{AAA}-NLS-GFP and phyA^{DDD}-NLS-GFP, the *PHYAp:PHYA*^{WT}*-GFP*, *PHYAp:PHYA*^{AAA}*-GFP* and *PHYAp:PHYA*^{DDD}*-GFP* constructs were first cut with *Not*I and *Bam*HI to release the *GFP* coding sequence. Then, PCR amplifications were performed using *35S:GFP-FHY1* (11) as the template and the primer pairs listed in Table S2 with the forward primer containing the coding sequence of the SV40 NLS (LQKKKRKVGG; 5), and then ligated into *Not*I/*Bam*HI-digested *PHYAp:PHYA*^{WT}*-GFP*, *PHYAp:PHYA*^{AAA}*-GFP* and *PHYAp:PHYA*^{DDD}*-GFP*, producing *PHYAp:PHYA*^{WT}*-NLS-GFP*, *PHYAp:PHYA*^{AAA}*-NLS-GFP* and *PHYAp:PHYA*^{DDD}*-NLS-GFP*, respectively.

To generate the PHYA^{WT}-BD, PHYA^{AAA}-BD and PHYA^{DDD}-BD constructs, the full-length coding sequences of PHYA, PHYA^{AAA} and PHYA^{DDD} were amplified by PCR using the pCF225 vector and the respective mutant constructs mentioned above as templates and the primer pairs listed in Table S2, and then cloned into the *Bam*HI and *Not*I sites of the D153 vector (12), respectively. To generate the AD-FHY1 and AD-FHL constructs, the full-length coding sequences of FHY1 and FHL were amplified by PCR with the primer pairs listed in Table S2, and then cloned into the *Eco*RI and *Xho*I sites of the pGADT7 vector (Clontech). To generate the construct expressing 6His-RPN6, the PCR fragment containing the full-length RPN6 open reading frame was cloned into the *Bam*HI and *Xho*I sites of the pET-28a vector (Novagen).

All of the primers used to generate the above-mentioned constructs are listed in Table S2, and all of the constructs were confirmed by sequencing prior to usage in the various assays.

Generation of Transgenic *Arabidopsis* Plants

To generate transgenic lines expressing various forms of WT and mutant phyA proteins,

the corresponding constructs were transformed into *Agrobacterium tumefaciens* (strain LBA4404) and then into *Arabidopsis phyA-1* mutants by the floral dip method (13). Transgenic plants were selected on Murashige & Skoog (MS) medium (Sigma) containing 50 mg/ml kanamycin solidified with 0.8% agar (Sigma). T2 plants showing 3:1 segregation for kanamycin resistance were considered single insertion lines and were selected for isolation of homozygous lines. Multiple independent homozygous lines for each construct were used for further studies.

Yeast Assays

For yeast two-hybrid assays, the respective combinations of GAL4 BD- and AD- fusion plasmids were cotransformed into the yeast strain Y187. For yeast three-hybrid assays, the respective combinations of plasmids were cotransformed into the yeast strain Y190. Yeast transformation was conducted as described in the Yeast Protocols Handbook (Clontech), and liquid assays using ONPG as the substrate were performed as described previously (12, 14).

Real-Time qRT-PCR

Total RNA was extracted from *Arabidopsis* seedlings using the RNeasy plant mini kit (TIANGEN). The cDNAs were synthesized from 1 μg total RNA using RevertAid First Strand cDNA Synthesis Kit (Thermo Fisher Scientific) according to the manufacturer's instructions. Real-time qPCR analysis was performed using PowerUp SYBR Green PCR Master Mix (Thermo Fisher Scientific) with a 7300 Real-Time PCR detection system (Thermo Fisher Scientific). qPCR was performed in triplicate for each sample, and the expression levels were normalized to that of a ubiquitin gene. The primers used for RT-qPCR are listed in Table S2.

Transcriptome Analyses

Total RNA was extracted by using the same procedures for qRT-PCR analysis. Sequencing was carried out with the Illumina HiSeq 2000 platform and the resulting reads were mapped to the reference genome of *Arabidopsis thaliana* (TAIR10) with

TopHat (http://tophat.cbcb.umd.edu) (15). Transcript expression was evaluated by cuffdiff (http://cufflinks.cbcb.umd.edu) (16), and transcript abundance was estimated by fragments per kilobase of exon model per million mapped fragments (FPKM). Differentially expressed genes were selected using Student's *t*-test with $P<0.05$ and fold change>2.

Nuclear-Cytoplasmic Fractionation

Nuclear fractionation was performed essentially as previously described (17) with the following modifications. Briefly, 1 g of *Arabidopsis* seedlings grown in darkness or continuous FR light for 4 d were ground into fine powder in liquid nitrogen, and then homogenized in 2 mL of pre-cooled (4°C) lysis buffer (20 mM Tris-HCl, pH 7.4, 25% Glycerol, 20 mM KCl, 2 mM EDTA, 2.5 mM $MgCl_2$, 250 mM Sucrose, 5 mM DTT) supplemented with 1× protease inhibitor cocktail (Roche), and filtered twice through two layers of Miracloth (Merck Millipore). The flow-through was spun 10 min at 2000*g*, 4°C, and the supernatant, consisting of the cytoplasmic fraction, was centrifuged 15 min at 13,000*g*, 4°C and collected. The pellet, containing the nuclear fraction, was washed five times with 2.5 mL of nuclear resuspension buffer NRBT (20 mM Tris-HCl, pH 7.4, 25% Glycerol, 2.5 mM $MgCl_2$ and 0.2% Triton X-100) and centrifuged 3 min at 1,500*g*, 4°C. The pellet was resuspended in 300 µL of pre-cooled NRBT2 (250 mM Sucrose, 10 mM Tris-HCl, pH 7.5, 10 mM $MgCl_2$, 1% Triton X-100, 0.035% β-mercaptoethanol) supplemented with 1× protease inhibitor cocktail (Roche), and carefully overlaid on top of 300 µL NRBT3 (1.7 M Sucrose, 10 mM Tris-HCl, pH 7.5, 2 mM $MgCl_2$, 0.15% Triton X-100, 0.035% β-mercaptoethanol) supplemented with 1× protease inhibitor cocktail (Roche). These were centrifuged at 16,000*g* for 45 min at 4°C, and the final nuclear pellet was resuspended in 2× SDS loading buffer. As quality controls for the fractionation, PEPC protein was used as the cytoplasmic marker, and histone H3 was used as the nuclear marker in immunoblot assays.

Immunoblotting

Arabidopsis seedlings were homogenized in extraction buffer containing 50 mM Tris-

HCl, pH 7.5, 10 mM $MgCl_2$, 150 mM NaCl, 1 mM EDTA, 10 mM NaF, 25 mM beta-glycerophosphate, 2 mM sodium orthovanadate, 10% (w/v) glycerol, 0.1% (w/v) Tween 20, 1 mM PMSF, 1× MG132, and 1× complete protease inhibitor cocktail (Roche). Immunoblotting was performed as previously described (11). Primary antibodies used in this study include anti-phyA (18), anti-FHY1 (11), anti-HY5 (9), anti-RPT5 (19), anti-GFP (Roche), anti-PEPC (Agrisera) and anti-H3 (Abcam) antibodies.

The anti-RPN6 polyclonal antibodies were made by Beijing Protein Innovation Co., Ltd. (BPI). 6His-RPN6 fusion proteins were first expressed in *Escherichia coli*, and then purified and used as antigens to immunize rabbits for the production of polyclonal antisera.

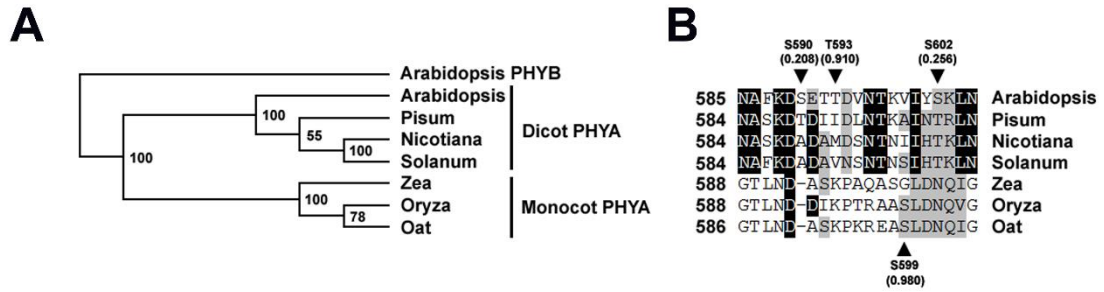

Fig. S1. Comparison of the hinge region sequences of monocot and dicot PHYA proteins.

(*A*) Phylogenetic analysis of PHYA protein sequences from monocots and dicots. The matrix of sequence similarities was calculated with the CLUSTAL program from the CLUSTAL W package (20), and the phylogenetic tree was constructed with the parsimony method using the PHYLIP package (21), with a bootstrap of 100 replicates. *Arabidopsis* PHYB sequence was used as an outgroup. (*B*) Alignment of the hinge region sequences of monocot and dicot PHYA proteins. Numbers at left indicate amino acid positions (from the translation start codon). The arrows on the top indicate the positions of *Arabidopsis* PHYA S590, T593 and S602, and the arrow at the bottom indicates the position of oat PHYA S599. NetPhos scores of S590, T593 and S602 of *Arabidopsis* PHYA and S599 of oat PHYA are shown.

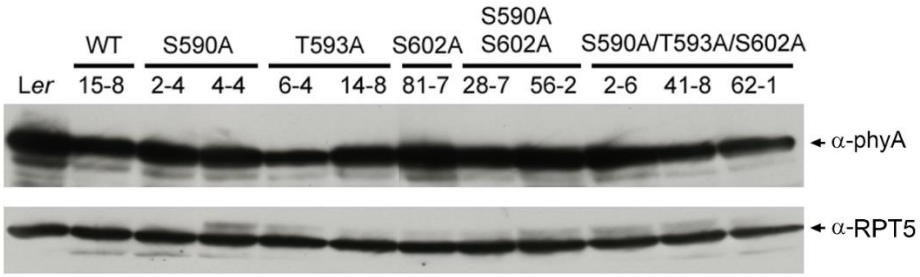

Fig. S2. Immunoblots showing phyA protein levels in the 4-d-old WT (L*er*) and homozygous transgenic lines expressing WT or various mutant forms of *Arabidopsis* phyA (S590, T593 and S602 mutated to alanines) grown in darkness. Anti-RPT5 was used as sample loading control.

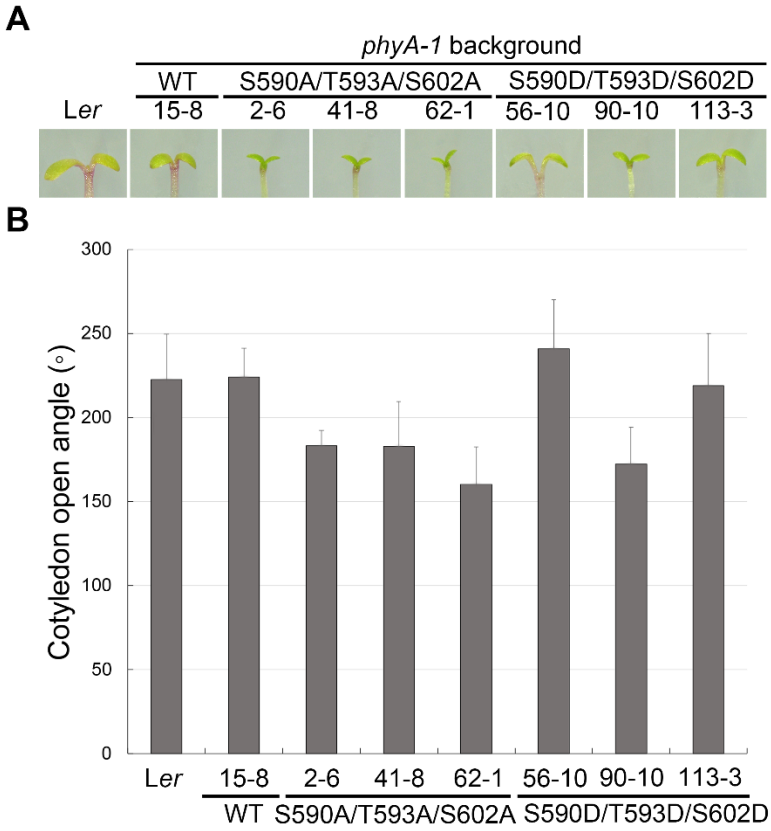

Fig. S3. Cotyledon open angles of phyA^{WT}, phyA^{AAA} and phyA^{DDD} lines. Phenotypes (*A*) and statistical analysis (*B*) of cotyledon open angles of 4-d-old WT (L*er*) and phyA^{WT}, phyA^{AAA} and phyA^{DDD} lines grown in continuous FR light. Error bars represent SD from 30 seedlings.

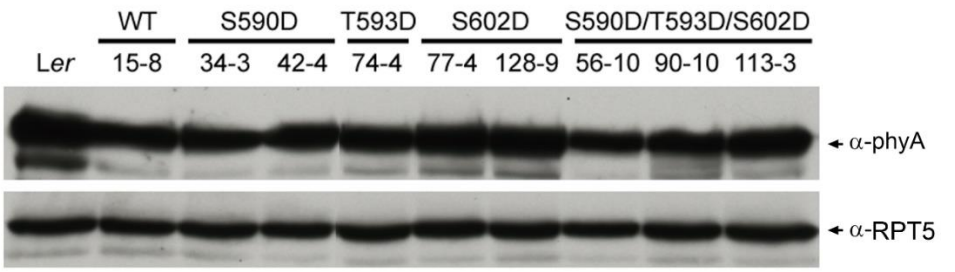

Fig. S4. Immunoblots showing phyA protein levels in the 4-d-old WT (L*er*) and homozygous transgenic lines expressing WT or various mutant forms of *Arabidopsis* phyA (S590, T593 and S602 mutated to aspartic acids) grown in darkness. Anti-RPT5 was used as sample loading control.

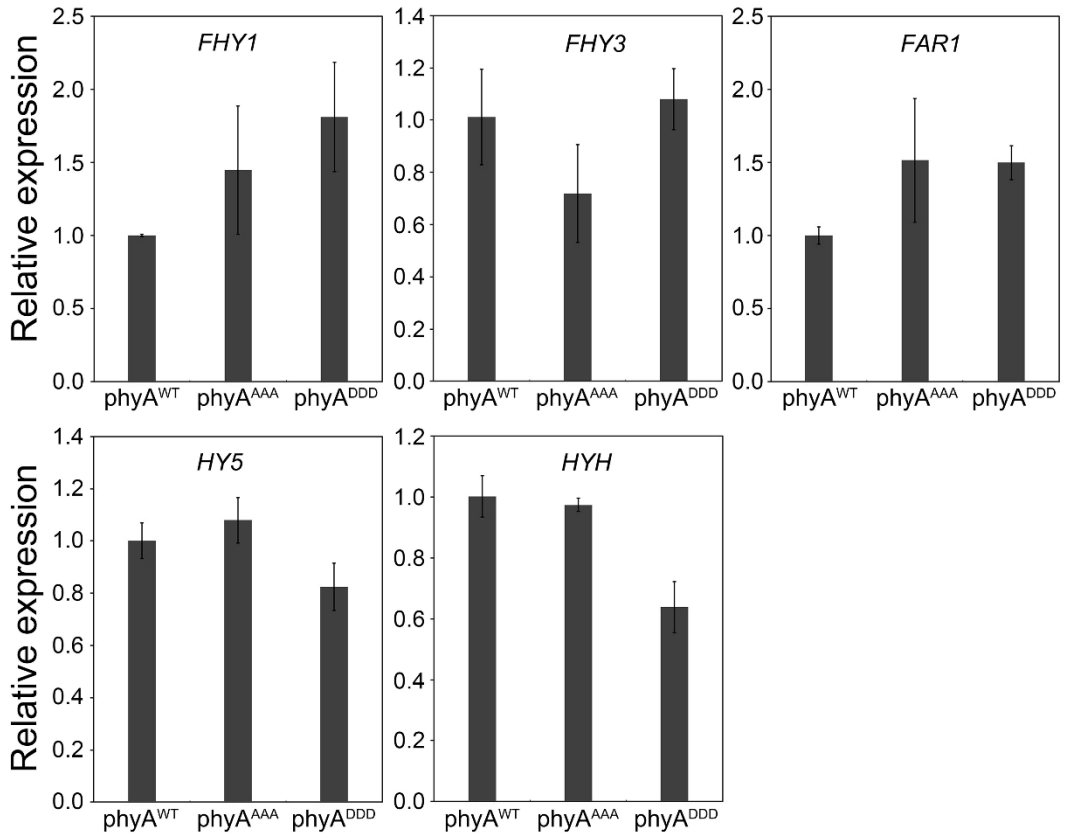

Fig. S5. The expression of several key regulatory genes of the phyA signaling pathway in phyA^{WT}, phyA^{AAA} and phyA^{DDD} seedlings.

qRT-PCR analyses showing the relative expression of *FHY1*, *FHY3*, *FAR1*, *HY5* and *HYH* in 4-d-old phyA^{WT}, phyA^{AAA} and phyA^{DDD} seedlings grown in FR light. Error bars represent SD of three technical replicates.

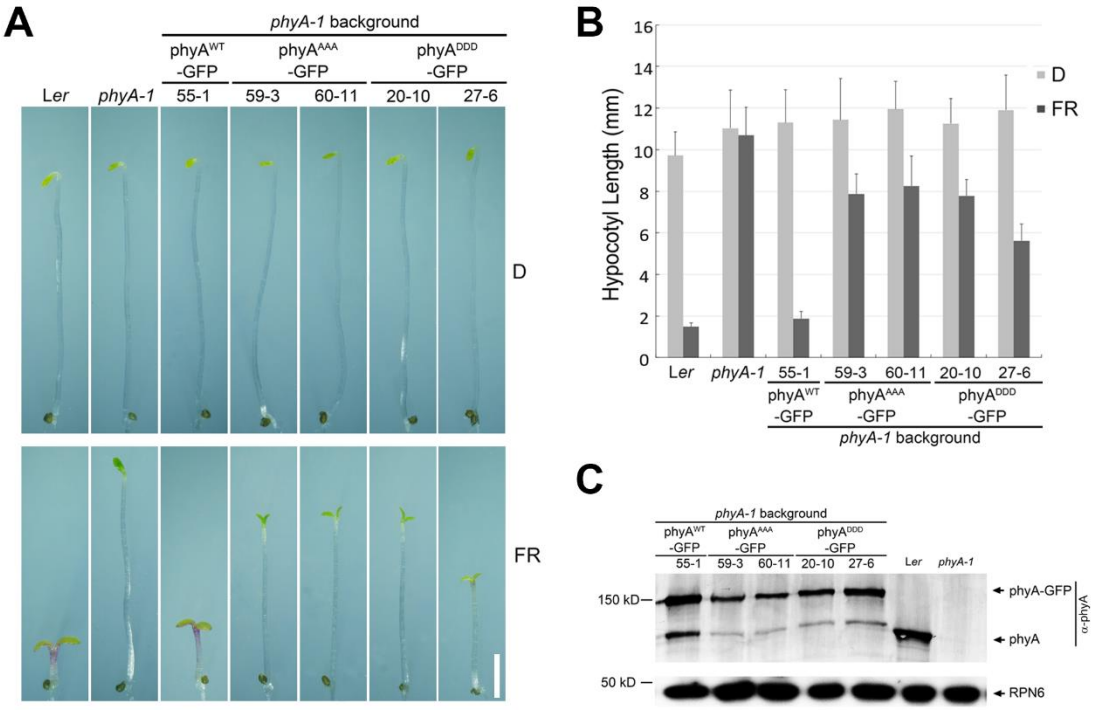

Fig. S6. Phenotypes and biochemical characterization of phyA^{WT}-GFP, phyA^{AAA}-GFP and phyA^{DDD}-GFP lines.

(*A*) Phenotypes of 4-d-old WT (L*er*), *phyA-1*, and homozygous *PHYAp:PHYA^{WT}-GFP phyA-1*, *PHYAp:PHYA^{AAA}-GFP phyA-1* and *PHYAp:PHYA^{DDD}-GFP phyA-1* seedlings grown in darkness (D) or continuous FR light. (Scale bar: 2 mm.) (*B*) Quantitative analysis of hypocotyl lengths of the WT (L*er*), *phyA-1*, and homozygous *PHYAp:PHYA^{WT}-GFP phyA-1*, *PHYAp:PHYA^{AAA}-GFP phyA-1* and *PHYAp:PHYA^{DDD}-GFP phyA-1* seedlings shown in (*A*). Error bars represent SD from 30 seedlings. (*C*) Immunoblots showing the protein levels of phyA^{WT}-GFP, phyA^{AAA}-GFP and phyA^{DDD}-GFP in 4-d-old WT (L*er*) and homozygous *PHYAp:PHYA^{WT}-GFP phyA-1*, *PHYAp:PHYA^{AAA}-GFP phyA-1* and *PHYAp:PHYA^{DDD}-GFP phyA-1* seedlings grown in darkness. Anti-RPN6 was used as a sample loading control.

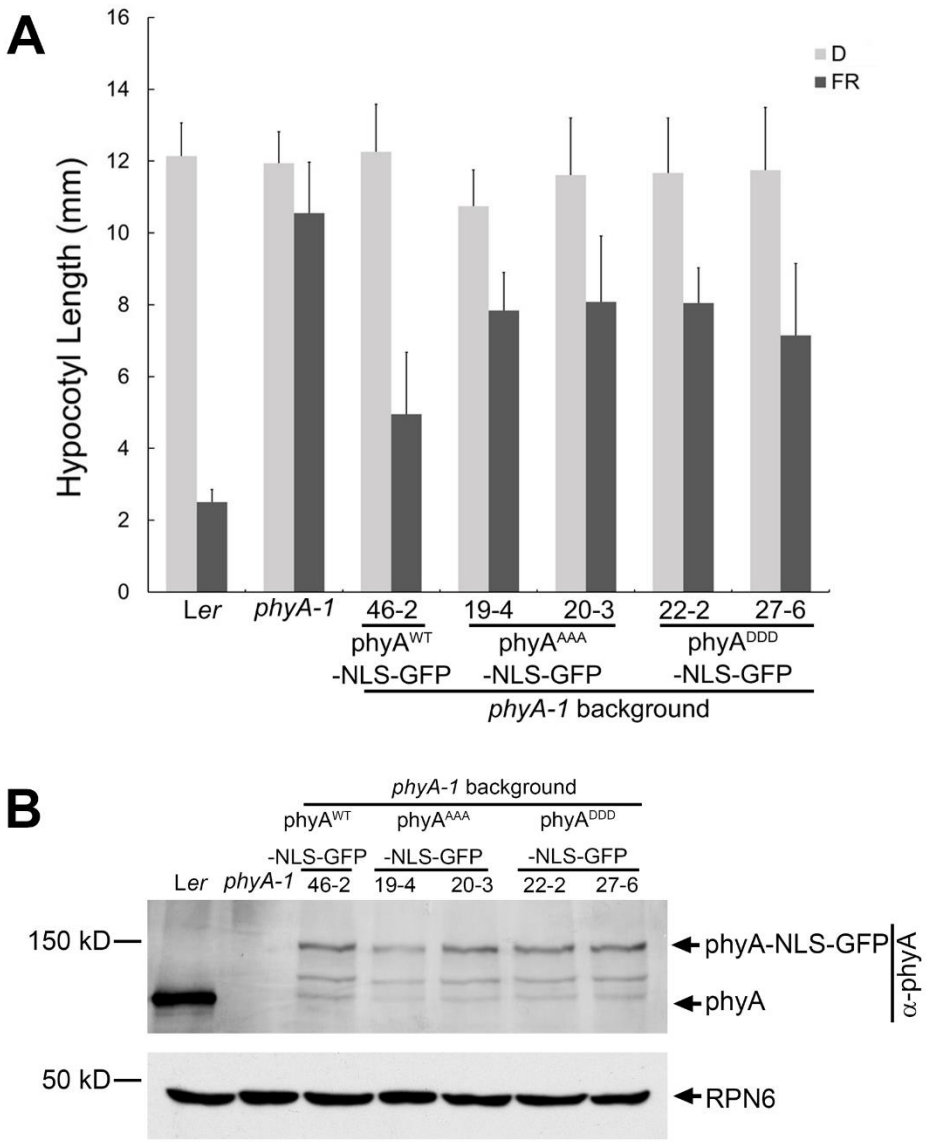

Fig. S7. Phenotypes and biochemical characterization of phyA^{WT}-NLS-GFP, phyA^{AAA}-NLS-GFP and phyA^{DDD}-NLS-GFP lines.

(*A*) Quantitative analysis of hypocotyl lengths of 4-d-old WT (L*er*), *phyA-1*, and homozygous *PHYAp:PHYA^{WT}-NLS-GFP phyA-1*, *PHYAp:PHYA^{AAA}-NLS-GFP phyA-1* and *PHYAp:PHYA^{DDD}-NLS-GFP phyA-1* seedlings grown in darkness (D) or continuous FR light. Error bars represent SD from 30 seedlings. (*B*) Immunoblots showing the protein levels of phyA^{WT}-NLS-GFP, phyA^{AAA}-NLS-GFP and phyA^{DDD}-NLS-GFP in 4-d-old WT (L*er*) and homozygous *PHYAp:PHYA^{WT}-NLS-GFP phyA-1*, *PHYAp:PHYA^{AAA}-NLS-GFP phyA-1* and *PHYAp:PHYA^{DDD}-NLS-GFP phyA-1* seedlings grown in darkness. Anti-RPN6 was used as sample loading control.

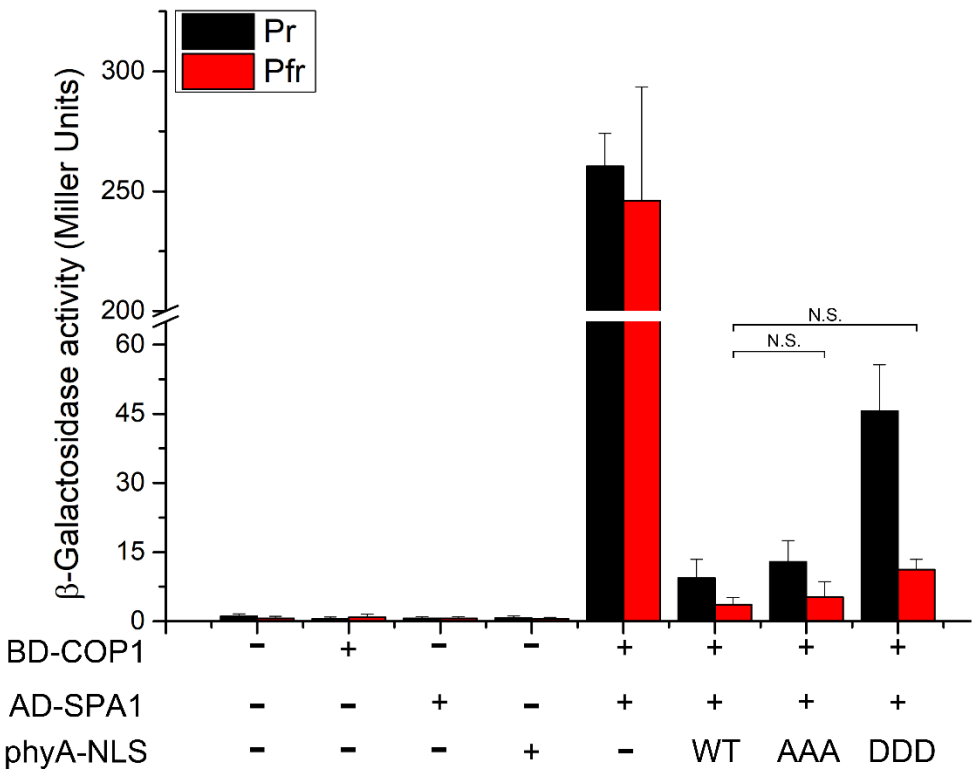

Fig. S8. The Pfr forms of both phyA^{AAA} and phyA^{DDD} displayed normal activities in inhibiting COP1-SPA1 interaction.

Yeast three-hybrid analyses of the effects of phyA^{WT}, phyA^{AAA} and phyA^{DDD} on the COP1-SPA1 interaction. phyA^{WT}-NLS, phyA^{AAA}-NLS and phyA^{DDD}-NLS were co-expressed with BD-COP1 and AD-SPA1 in the yeast strain Y190. The yeast cells were grown in liquid SD medium supplemented with 10 μM PCB in darkness (the Pr form) or irradiated with 5 min of R (30 μmol m^{-2} s^{-1}) twice (the Pfr form), and the interaction of BD-COP1 and AD-SPA1 was examined, respectively, by liquid culture assays using ONPG as the substrate. Values are the average data of four independent yeast clones. Error bars represent SD. N.S., not significant.

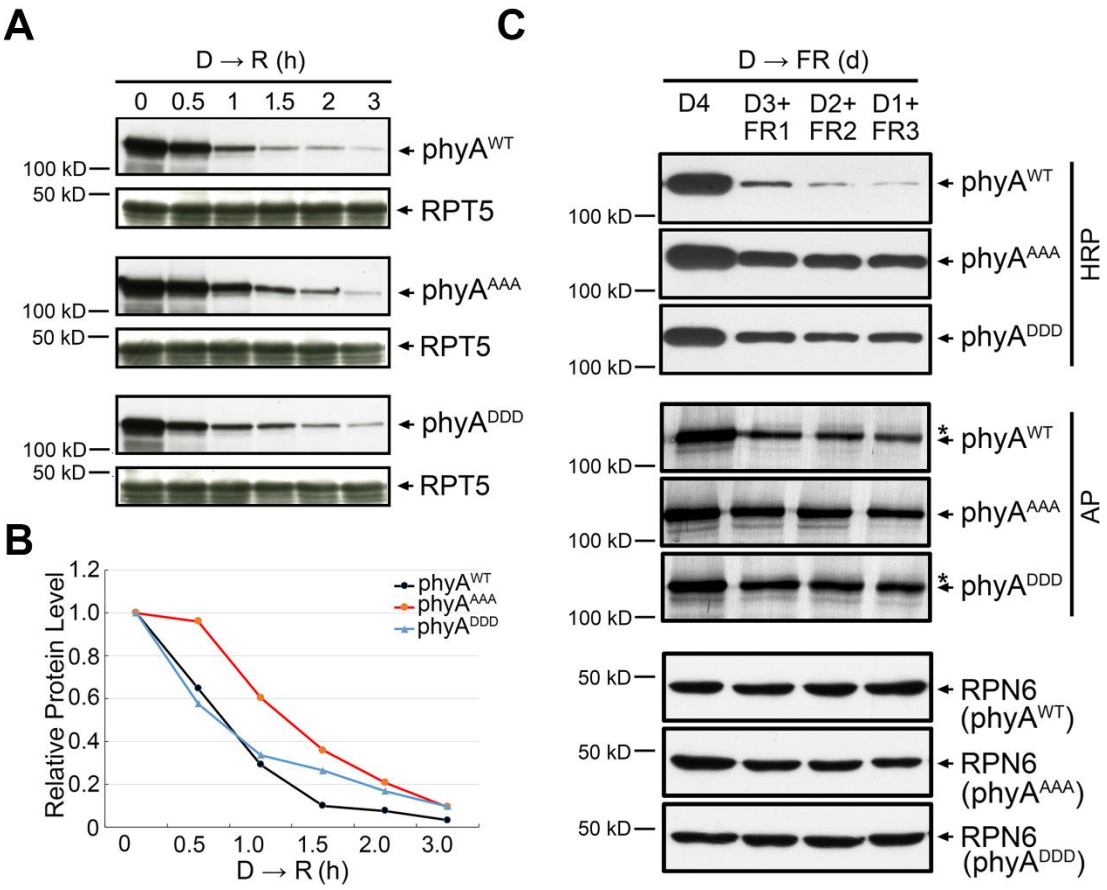

Fig. S9. Both phyA^{AAA} and phyA^{DDD} are degraded more slowly than phyA^{WT} upon light illumination.

(*A*) Immunoblots showing the degradation of phyA^{WT}, phyA^{AAA} and phyA^{DDD} upon exposure to R light. Homozygous *PHYAp:PHYA^{WT} phyA-1*, *PHYAp:PHYA^{AAA} phyA-1* and *PHYAp:PHYA^{DDD} phyA-1* seedlings were grown first in darkness (D) for 4 days, and then irradiated with R light for various time points. Anti-RPT5 was used as sample loading control. (*B*) Quantification of phyA^{WT}, phyA^{AAA} and phyA^{DDD} protein levels shown in (*A*) normalized to RPT5. The phyA^{WT}, phyA^{AAA} and phyA^{DDD} protein levels before irradiation were set as 1.0. (*C*) Immunoblots showing the phyA^{WT}, phyA^{AAA} and phyA^{DDD} protein levels when the homozygous *PHYAp:PHYA^{WT} phyA-1*, *PHYAp:PHYA^{AAA} phyA-1* and *PHYAp:PHYA^{DDD} phyA-1* seedlings were grown in darkness for days (D4), or in darkness first for 1 to 3 days and then transferred to FR light for up to 4 days. The seedlings were harvested simultaneously and then subjected to immunoblotting. HRP, horseradish peroxidase (HRP) conjugated secondary antibody and detection system were employed; AP, alkaline phosphatase

(AP) conjugated secondary antibody and detection system were employed. Anti-RPN6 was used as a sample loading control. For the data obtained by the AP system, the asterisk and arrowhead represent the phosphorylated and unphosphorylated phyA forms, respectively (22).

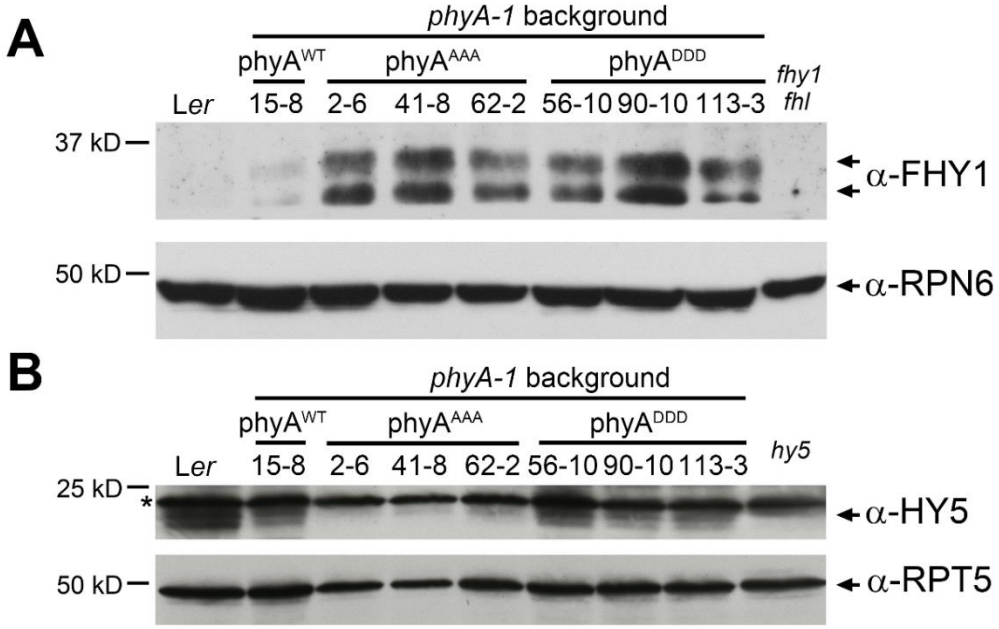

Fig. S10. Altered accumulation of FHY1 and HY5 proteins in phyA^{AAA} and phyA^{DDD} lines.

(*A*) Immunoblots showing FHY1 protein levels in 4-d-old WT (L*er*) and homozygous *PHYAp:PHYA^{WT} phyA-1*, *PHYAp:PHYA^{AAA} phyA-1* and *PHYAp:PHYA^{DDD} phyA-1* seedlings grown in continuous FR. The *fhy1 fhl* mutant plants were included as the negative control. Anti-RPN6 was used as sample loading control. (*B*) Immunoblots showing HY5 protein levels in 4-d-old WT (L*er*) and homozygous *PHYAp:PHYA^{WT} phyA-1*, *PHYAp:PHYA^{AAA} phyA-1* and *PHYAp:PHYA^{DDD} phyA-1* seedlings grown in continuous FR. The *hy5* mutant plants were included as the negative control. Anti-RPT5 was used as sample loading control.

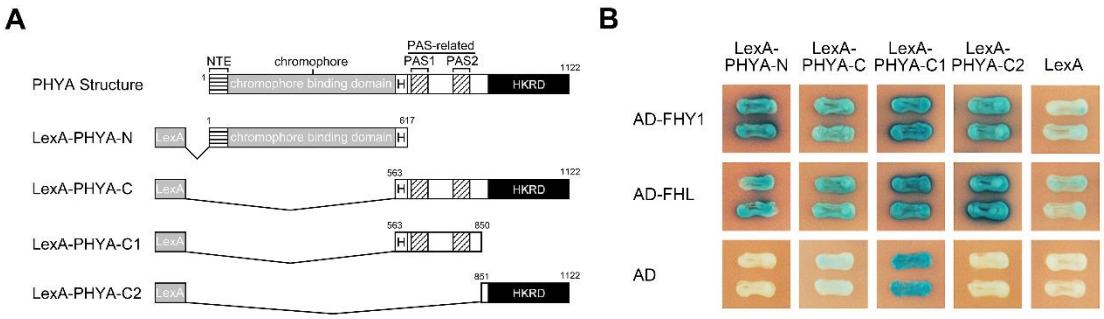

Fig. S11. Both N- and C-terminal domains of PHYA interact with FHY1 and FHL. (*A*) Schematic diagram of bait proteins (PHYA-N, PHYA-C, PHYA-C1, and PHYA-C2 fused with LexA DNA binding domains). NTE, N-terminal extension; HKRD, histidine kinase-related domain; H, hinge. (*B*) Yeast two-hybrid assays showing that both N- and C-terminal domains of PHYA interact with FHY1 and FHL.

Other Supporting Information Files

Table S1. Summary of *Arabidopsis phyA* mutant alleles caused by single amino acid substitutions.

Table S2. Summary of primers used in this study.

Dataset S1. List of genes whose expression was changed in both phyA^{AAA} and phyA^{DDD} lines in FR light.

References

1. Whitelam GC, et al. (1993). Phytochrome A null mutants of *Arabidopsis* display a wild-type phenotype in white light. *Plant Cell* 5:757-768.
2. Fry RC, Habashi J, Okamoto H, Deng XW (2002) Characterization of a strong dominant phytochrome A mutation unique to phytochrome A signal propagation. *Plant Physiol* 130:457-465.
3. Rosler J, Klein I, Zeidler M (2007) Arabidopsis *fhl/fhy1* double mutant reveals a distinct cytoplasmic action of phytochrome A. *Proc Natl Acad Sci USA* 104:10737-10742.
4. Oyama T, Shimura Y, Okada K (1997) The *Arabidopsis HY5* gene encodes a bZIP protein that regulates stimulus-induced development of root and hypocotyl. *Genes Dev* 11:2983-2995.
5. Genoud T, et al. (2008) FHY1 mediates nuclear import of the light-activated phytochrome A photoreceptor. *PLoS Genet* 4:e1000143.
6. Rausenberger J, et al. (2011) Photoconversion and nuclear trafficking cycles determine phytochrome A's response profile to far-red light. *Cell* 146:813-825.
7. Xu Y, Parks BM, Short TW, Quail PH (1995) Missense mutations define a restricted segment in the C-terminal domain of phytochrome A critical to its regulatory activity. *Plant Cell* 7:1433-1443.
8. Lin R, et al. (2007) Transposase-derived transcription factors regulate light signaling in *Arabidopsis*. *Science* 318:1302-1305.
9. Li J, et al. (2010) *Arabidopsis* transcription factor ELONGATED HYPOCOTYL5

plays a role in the feedback regulation of phytochrome A signaling. *Plant Cell* 22:3634-3649.

10. Trupkin SA, Debrieux D, Hiltbrunner A, Fankhauser C, Casal JJ (2007) The serine-rich N-terminal region of *Arabidopsis* phytochrome A is required for protein stability. *Plant Mol Biol* 63:669-678.
11. Shen Y, et al. (2005) *Arabidopsis* FHY1 protein stability is regulated by light via phytochrome A and 26S proteasome. *Plant Physiol* 139:1234-1243.
12. Shimizu-Sato S, Huq E, Tepperman JM, Quail PH (2002) A light-switchable gene promoter system. *Nat Biotechnol* 20:1041-1044.
13. Clough SJ, Bent AF (1998) Floral dip: a simplified method for Agrobacterium-mediated transformation of *Arabidopsis thaliana*. *Plant J* 16:735-743.
14. Sheerin DJ, et al. (2015) Light-activated phytochrome A and B interact with members of the SPA family to promote photomorphogenesis in *Arabidopsis* by reorganizing the COP1/SPA complex. *Plant Cell* 27:189-201.
15. Kim D, et al. (2013) TopHat2: accurate alignment of transcriptomes in the presence of insertions, deletions and gene fusions. *Genome Biol* 14:R36
16. Trapnell C, et al. (2013) Differential analysis of gene regulation at transcript resolution with RNA-seq. *Nat Biotechnol* 31:46-53.
17. Wang W, et al. (2011) An importin beta protein negatively regulates MicroRNA activity in *Arabidopsis*. *Plant Cell* 23:3565-3576.
18. Shen Y, et al. (2009) Phytochrome A mediates rapid red light-induced phosphorylation of *Arabidopsis* FAR-RED ELONGATED HYPOCOTYL1 in a low fluence response. *Plant Cell* 21:494-506.
19. Kwok SF, Staub JM, Deng XW (1999) Characterization of two subunits of *Arabidopsis* 19S proteasome regulatory complex and its possible interaction with the COP9 complex. *J Mol Biol* 285:85-95.
20. Thompson JD, Higgins DG, Gibson TJ (1994) CLUSTAL W: improving the sensitivity of progressive multiple sequence alignment through sequence weighting, position-specific gap penalties and weight matrix choice. *Nucleic acids Res* 22:4673-4680.

21. Felsenstein J (1989) PHYLIP: Phylogeny Interence Package (Version 3.2). *Cladistics 5*:164–166.
22. Saijo Y, et al. (2008) *Arabidopsis* COP1/SPA1 complex and FHY1/FHY3 associate with distinct phosphorylated forms of phytochrome A in balancing light signaling. *Mol Cell* 31:607-613.

Table S1. Summary of *Arabidopsis phyA* mutant alleles caused by amino acid substitutions.

No	Allele Names	Amino acid substitutions	Residues conserved or not	References
1	*phyA-103-1*	G727E	Yes	Xu et al. (1995), Plant Cell, 7:1433-1443
2	*phyA-103-2*	G727E	Yes	Xu et al. (1995), Plant Cell, 7:1433-1443
3	*phyA-103-3*	G727E	Yes	Xu et al. (1995), Plant Cell, 7:1433-1443
4	*phyA-104*	P632S	Yes	Xu et al. (1995), Plant Cell, 7:1433-1443
5	*phyA-105*	A893V	Yes (A or S)	Xu et al. (1995), Plant Cell, 7:1433-1443
6	*phyA-106*	C716Y	Yes	Xu et al. (1995), Plant Cell, 7:1433-1443
7	*phyA-107*	E119K	Yes (D or E)	Xu et al. (1995), Plant Cell, 7:1433-1443
8	*phyA-108*	G768D	Yes	Xu et al. (1995), Plant Cell, 7:1433-1443
9	*phyA-109*	G367S	Yes	Xu et al. (1995), Plant Cell, 7:1433-1443
10	*phyA-110*	R279S	Yes	Xu et al. (1995), Plant Cell, 7:1433-1443
11	*phyA-205*	V631M	Yes	Reed et al. (1994), Plant Physiol, 104:1139-1149
12	*phyA-300D*	V631M	Yes	Fry et al. (2002), Plant Physiol, 130:457-465
13	*phyA-5*	A30V	Yes	Sokolova et al. (2012), Plant Physiol, 158:107-118
14	*eid4*	E229K	Yes	Dieterle et al. (2005), Plant J, 41:146-161
15	*Lm-2*	M548T	Yes	Maloof et al. (2001), Nat Genet, 29:441-446

Table S2. Summary of primers used in this study.

Purpose		Primer Sequence (5'-3')
Plasmid Constructs (Note: The underlined nucleotides indicate the restriction sites for cloning.)		
Site-directed Mutagenesis	S590A	CTTATTTTGAGGAATGCTTTCAAGGATGCTGAAACTACT GATGTGAATACAA
		TTGTATTCACATCAGTAGTTTCAGCATCCTTGAAAGCAT TCCTCAAAATAAG
	T593A	GCTTTCAAGGATAGTGAAACTGCTGATGTGAATACAAA GGTCA
		TGACCTTTGTATTCACATCAGCAGTTTCACTATCCTTGA AAGC
	S602A	GATGTGAATACAAAGGTCATTTACGCGAAGCTAAATGA TCTCAAAATT
		AATTTTGAGATCATTTAGCTTCGCGTAAATGACCTTTGT ATTCACATC
	S590D	GAGGAATGCTTTCAAGGATGATGAAACTACTGATGTGA ATAC
		GTATTCACATCAGTAGTTTCATCATCCTTGAAAGCATTC CTC
	T593D	CTTTCAAGGATAGTGAAACTGATGATGTGAATACAAAG GTCA
		TGACCTTTGTATTCACATCATCAGTTTCACTATCCTTGAA AG
	S602D	GTGAATACAAAGGTCATTTACGATAAGCTAAATGATCTC AAAATT
		AATTTTGAGATCATTTAGCTTATCGTAAATGACCTTTGT ATTCAC
PHYAp:PHYA-GFP	PHYA	ATTGGACTAGTAAAAATGTCAGGCTCTAGGCCGACTC
		ATTGGGGATCCAAAGCGGCCGCCTTGTTTGCTGCAGCGA GTTCC
	GFP	ATTGGGCGGCCGCAATGGGTAAAGGAGAACTTTTC
		ATTGGGGATCCCTAGATAGATCTGTATAGTTCATCCAT
phyA-NLS-GFP	NLS-GFP	ATTCGGGCGGCCGCATTGCAGAAAAAGAAGAGAAAGGT CGGTGGAGCAGCTGCGATGGGTAAAGGAGAACTTTTC
		ATTGGGGATCCCTAGATAGATCTGTATAGTTCATCCAT
Yeast Two Hybrid	PHYA-BD	AAGGAAGGATCCAAAATGTCAGGCTCTAGGCCGAC
		AAGGAAGCGGCCGCTTCTTGTTTGCTGCAGCGAGTTC
	AD-FHY1	TGGATCGAATTCATGCCTGAAGTGGAAGTGGATA
		TGGATCCTCGAGTTACAGCATTAGCGTTGAGAAGTAT
	AD-FHL	TGGATCCAATTGATGGATGATGCAGATAAGAG
		TGGATCCTCGAGTTACATCATGAGTGTAGAAAAGTAC
Antibody		
6His fusions (pET28a vector)	RPN6	GCGTGGATCCATGGTTTCCTATCGTGCTAC
		GCGTCTCGAGGGACATGATTTTGGCAG

Real-time qRT-PCR		
Several representative genes of RNA-seq data	PIN5	CCGCTCTTCACCATTGAGTT
		GCTATATTTGGCCCACAACG
	EARLI1	GAAAGGTTCCGTCTGGCTTC
		AAAGTCTCACTCTCACACATTGG
	AT1G52100	GGAGTCCATGTCACGGCTAT
		TCGGATTGATACAACATTACCTT
	PME35	TGAACCTCTTGTCCCTTCAGA
		ATCGGAGTTTGGGTGTCTTG
	WSD1	AGCCTCTTAGCCCAATGTCA
		GATCGGTTGCATCGAGTTTT
	BHLH038	GGCCGTCAACGAATCAATAC
		GACGAAACAGATACTCCCAAGC
Key regulatory genes of the phyA signaling pathway	FHY3	GGTAGGAGAACATGTGCGAA
		TATGCTCCCTCACAAAGCTG
	FAR1	GACATTCTGCATGCGGTTAG
		GCTGACATCGGTCTGAAGAA
	FHY1	GATGAAAGAGGAATCATCTGGA
		AATCCTCTAAGTTCTGAGTCCCA
	HY5	CCATCAAGCAGCGAGAGGTCATCAA
		CGCCGATCCAGATTCTCTACCGGAA
	HYH	CCCACAAGAAGCACAAAACTGAGGAAA
		CTTCCACGGCGGCGTTTAGCTGTAGAGA
Internal control genes	UBQ	TTCCTTGATGATGCTTGCTC
		TTGACAGCTCTTGGGTGAAG